



ELSEVIER

Available online at www.sciencedirect.com

SCIENCE @ DIRECT®

Proceedings of the Combustion Institute 30 (2005) 2105–2112

Proceedings
of the
Combustion
Institute

www.elsevier.com/locate/proci

Flame structure of HMX/GAP propellant at high pressure

Alexander A. Paletsky^a, Oleg P. Korobeinichev^{a,*},
Alexander G. Tereshchenko^a, Evgeny N. Volkov^b, Pavel D. Polyakov^b

^a *Institute of Chemical Kinetics and Combustion, Siberian Branch of Russian Academy of Sciences,
Novosibirsk 630090, Russia*

^b *Novosibirsk State University, Novosibirsk 630090, Russia*

Abstract

The chemical and thermal structure of a HMX/GAP propellant flame was investigated at a pressure of 0.5 MPa using molecular beam mass spectrometry and a microthermocouple technique. The pressure dependence of the burning rate was measured in the pressure range of 0.5–2 MPa. The mass spectrometric probing technique developed for flames of energetic materials was updated to study the chemical structure of HMX/GAP flames at high pressures. Eleven species, including HMX vapor, were identified, and their concentrations were measured in a zone adjacent to the burning surface at pressures of 0.5 and 1 MPa. Temperature profiles in the propellant combustion wave were measured at pressures of 0.5 and 1 MPa. Species concentration profiles were measured at 0.5 MPa. Two main zones of chemical reactions in the flame were found. The data obtained can be used to develop and validate combustion models for HMX/GAP propellants.

© 2004 The Combustion Institute. Published by Elsevier Inc. All rights reserved.

Keywords: HMX; GAP; Nitramine propellant; Flame structure; High pressure

1. Introduction

Studies of the combustion mechanism of composite propellants (CPs) based on cyclic nitramines (HMX and RDX) with glycidyl azide polymer (GAP) as an active binder are of both practical and theoretical interest [1,2]. Practical interest is motivated by the use of energetic materials (EMs) to improve the ballistic characteristics of propellants. A realistic propellant combustion model should be based on knowledge of the actual

physicochemical processes in the propellant condensed phase and its ingredients, and the detailed kinetic mechanism of reactions in CP flames. The combustion mechanisms of the HMX/GAP ingredients have been extensively studied [1–4]. The thermal structure of the self-sustained combustion wave of HMX/GAP (80/20 wt%) propellant over a wide pressure range has been more thoroughly investigated using the microthermocouple technique [1,3]. Kubota and Sonobe [1] found the existence of a dark zone ~0.5 mm wide near the burning surface of cured HMX/GAP propellant (for GAP with a molecular weight (MW_{GAP}) of 2000) at a pressure of 0.5 MPa. Zenin and Finjakov [3] determined the main characteristics of the HMX/GAP ($MW_{GAP} = 2000$) combustion

* Corresponding author. Fax: +7 3832 342350.

E-mail address: korobein@ns.kinetics.nsc.ru (O.P. Korobeinichev).

wave at pressures of 0.5–10 MPa and different initial temperatures. Bimodal HMX was used in these investigations. The bimodal HMX particle size distribution was as follows: 70% of the particles with a size of 2 μm and 30% of 20 μm in [1], and 50% of the particles smaller than 50 μm and 50% with sizes of 150–300 μm in [3]. A plateau on the temperature profiles in the dark zone was revealed in both studies [1,3]. Litzinger et al. [4] investigated the chemical structure of the flame of a HMX (75 μm)/GAP ($MW_{\text{GAP}} \sim 5500$) propellant at laser-supported combustion at atmospheric pressure using microprobe mass spectrometry. They measured the concentration profiles of the main combustion species (except for H_2 and HMX vapor). Three zones of chemical reactions were observed. In the first zone 0.5 mm wide, complete consumption of NO_2 , a slight increase in the NO and H_2O concentrations, and a decrease in the CH_2O concentration took place. In the second (dark) zone 3–3.5 mm wide, the concentrations of HCN , NO , CO , N_2O , CO_2 , and N_2 did not change or changed only slightly. In the third (luminous) zone, the concentrations of all species (except for H_2O) changed abruptly. Yang and co-workers [2] developed a model for HMX/GAP combustion over broad ranges of ambient pressure, laser intensity, and propellant composition. The model includes four global condensed phase decomposition reactions of HMX and GAP, and a detailed gas-phase chemical kinetics mechanism involving 74 species and 532 reactions. A comparison of the calculation results of [2] with experimental data on the flame structure of laser-assisted combustion [4] showed that they are in fairly good agreement for some of the main species. However, the model in question does not describe the presence of high NO_2 and CH_2O concentrations near the burning surface observed in [4]. On the other hand, the model of [2] predicts the presence of HMX vapor in a narrow zone near the surface, while in the experiment, HMX vapor was not observed. It was shown earlier [5,6] that in laser-assisted and self-sustained combustion, some EMs (RDX, HMX) have different flame structures. Thus, it is not possible to model self-sustained combustion using the results obtained for laser-assisted combustion. There are no experimental data on the chemical structure of flame for the self-sustained combustion of HMX/GAP propellant at high pressures (0.5 MPa and higher). The goal of the present paper was to make up for this deficiency. Such data are needed to develop a model for the self-sustained combustion of this propellant.

2. Experimental

The HMX/GAP (80/20 wt%) flame structures at pressures of 0.5 and 1 MPa were investigated

using mass spectrometric probing (MSP) of flames of energetic materials (EMs) with molecular beam sampling (MBS) described in [7], a microthermocouple technique, and video recording. In MSP of EM flames, the burning strand moves toward the probe at a rate exceeding the propellant burning rate with simultaneous sampling of all combustion zones, including the zone adjacent to the burning surface. The system of molecular beam sampling of EM flames detects both stable species and unusual species such as EM vapors. A time-of-flight mass spectrometer (TOFMS) was used to measure mass spectra of samples.

GAP was synthesized and certified at St. Petersburg Technological University. The brutto formula of GAP is: $\text{C}_{60}\text{H}_{104}\text{O}_{21}\text{N}_{54}$. Density of GAP is 1.275 g/cm^3 . Enthalpies of formation of GAP and HMX are equal to 146 and 71 kcal/kg [8], respectively. Therefore, enthalpy of formation of the propellant is equal to 86 kcal/kg, and calculated density of the propellant—1.73 g/cm^3 . Propellant samples were prepared by mixing a bimodal crystal HMX powder (a coarse fraction with a particle size of 150–250 μm and a fine fraction with particle sizes less than 20 or 50 μm in a 50/50 wt% ratio) and GAP ($MW \sim 2000$). The mixture was prepared in dry air and was then evacuated before sample preparation. The sample density was equal to $1.69 \pm 0.01 \text{ g}/\text{cm}^3$ ($\sim 98\%$ of the calculated density).

Experiments on combustion of uncured HMX/GAP propellants at pressures of 0.5–2 MPa were conducted in a high-pressure combustion chamber in an argon atmosphere. Propellant burning rates were determined by visualization of the motion of the propellant burning surface using video recording.

The thermal structure of uncured HMX/GAP propellant flame at 0.5 and 1 MPa was investigated using Π -shaped WRe (5%)–WRe (20%) ribbon thermocouples embedded in sample. The temperature of the final combustion products was corrected for heat loss by radiation [9]. The thermocouples were made by rolling wires of diameters 15 and 50 μm . The thermocouples had a thickness (h) of ~ 6 and 15 μm , and length of shoulders (l) of 1.2 and 3.0 mm at 0.5 and 1 MPa, respectively. The ratio l/h in our experiments was equal to ~ 200 . The calculations in [10] show that at this l/h ratio, the temperature measurement error due to heat losses in the thermocouple shoulders does not exceed 2%. To prevent flame propagation along the side surface, the samples were placed in cylinders ($\varnothing = 6$ mm, length ~ 6 mm) made of thin cigarette paper treated by an aqueous solution of ammonium perchlorate. This provided for even combustion and did not prevent observation of the thermocouple at the moment it appeared in the gas phase. The temperature error in a single experiment was ± 25 K. The scatter in the temperatures of the final

combustion products measured in different experiments was equal to ± 50 K. The strand was ignited by an electrically heated Nichrome wire placed at 0.5–1 mm above the sample surface. Quartz “sonic” probes with different wall thicknesses (Δr) and with orifice diameter of 30–40 μm were used for sampling. The opening angle of the internal cone of the probes was equal to $\sim 40^\circ$. Three types of probes were used: a thick-walled ($\Delta r = 1.4$ mm) probe with additional heating similar to that described in [11] (Probe 1); a thick-walled probe with wall thickness near the probe orifice less than in Probe 1 ($\Delta r = 0.35$ mm) without additional heating (Probe 2); and a thin-walled probe ($\Delta r = 0.17$ mm) without additional heating (Probe 3). The main goal of using the probe with additional heating was to increase the temperature of the probe tip to a value slightly higher than the temperature of the propellant burning surface (603 K [3]). This prevented plugging of the probe orifice due to HMX vapor condensation on the inner walls of the probe near its tip. At the same time, this allowed detection of HMX vapor in the low-temperature flame zone near the burning surface.

Preliminary experiments with probes of different wall thicknesses allowed us to determine the maximum time of sampling from HMX/GAP flame during which fusion of the orifice of the probe or failure of the probe did not occur. In measurements of species concentration profiles, the height of samples varied from 2 to 4 mm, and diameter—from 3 to 8 mm. Quartz probes of different types became unfit, on the average, after four or five experiments. In the case of Probes 1 and 2, failure of the probe orifice occurred if the residence time of the probe in flame exceeded 2 s. For Probe 3, the residence time in flame should not exceed 0.6 s.

Calibration [12] of MBMS for species H_2 , H_2O , HCN, N_2 , CO, NO, CH_2O , N_2O , NO_2 , CO_2 , and HMX vapor (HMX_v) was conducted in a flow reactor at constant pressures of 0.3–0.4 MPa. In the calibration, the gas temperature and the temperature of the probe tip were in the range of ~ 573 –623 K. The experimental temperature of the final combustion products was very close to the calculated temperature at thermodynamic equilibrium (equilibrium was calculated using REAL code [13]). Therefore, the composition of the final combustion products should be very close to the calculated composition at thermodynamic equilibrium. With this assumption, the calibration coefficients for the final combustion products (H_2 , H_2O , N_2 , CO, and CO_2) were determined using measured intensities of mass peaks (2, 14, 18, 22, 28, and 44) and the calculated composition at thermodynamic equilibrium. Comparison of the thus obtained calibration coefficients with results of direct measurements shows

that they coincide with good accuracy (except for CO_2). It was difficult to obtain a correct experimental calibration coefficient for CO_2 because this gas readily forms clusters during expansion in the probe nozzle. Therefore, in the case of CO_2 , we used the calibration coefficient calculated using the composition at thermodynamic equilibrium. The calculated coefficients (for H_2 , H_2O , N_2 , CO, and CO_2) and measured coefficients for other species were used to determine the combustion product composition near the burning surface. The measurement accuracy of the mole fractions of the final combustion products (H_2O , H_2 , O_2 , N_2 , and CO) was about 10%. The mole fractions of HCN, O_2 , N_2O , NO, NO_2 , and HMX vapor near the burning surface were measured with an accuracy of about 15%, and the mole fractions of CH_2O , N_2 , and CO with an accuracy of about 30%. To identify HMX vapor, we performed special experiments on HMX decomposition (evaporation) in an Ar flow at 0.1 MPa using a flow reactor similar to that described in [12] and Probe 1. Drops of an HMX solution in acetone were applied on the central part of a metal ribbon used as a heater. As acetone evaporates, HMX crystals with sizes less than 0.04 mm formed on the heater surface. The sample weight was less than 1 mg. The temperature of the probe tip was 573 K, as in the experiments with flame probing. The plate was heated by an electric current at a heating rate of 700 K/s up to the melting point of HMX (553 K) and then at a heating rate of about 75 K/s. The mass spectrum obtained under these conditions did not contain a mass peak at $m/e = 44$, and the intensity of the mass peak at $m/e = 42$ was maximal. This agrees with the data of Behrens [14] (Table 1), who observed HMX vapors in HMX decomposition in a Knudsen cell at a pressure of $\sim 10^{-2}$ Torr. However, there are some discrepancies in the intensities of mass peaks 30 and 75. They are likely due to different experimental conditions, including the system for delivering sampled gas to the ion source of the mass spectrometer.

In HMX calibration with increase in the mass peak intensities of HMX vapor (ΔI_{HMX}), the mass peak intensities of the carrier gas decrease (ΔI_{Ar}). For HMX vapor, the calibration coefficient was determined from the formula: $K_{\text{HMX/Ar}} = \Delta I(42)_{\text{HMX}}/\Delta I(40)_{\text{Ar}}$. $I(42)$ is the intensity of mass peak 42, which is the largest peak in the mass spectrum of HMX.

Table 1
Mass spectra of HMX vapor

	29	30	42	46	75
HMX [14]	14.7	25.5	100	65.4	51.4
HMX	15	71	100	62	37

3. Results and discussions

3.1. Burning rate

Burning rate versus pressure relationships for pure HMX and uncured HMX/GAP propellants obtained by different investigators (Kubota and Sonobe [1] and Zenin and Finjakov [3]), including our data, are presented in Fig. 1. The burning rates of pure HMX over the pressure range of 0.5–2 MPa are higher than those of HMX-based propellants with active binder GAP. There is scatter in burning rate data for cured and uncured propellants. Cured propellants based on fine bimodal HMX [1] burned at the same rate as uncured propellants with coarse bimodal HMX [3]. According to Zenin [15], curing of GAP in HMX/GAP propellant leads to an increase in the burning rate and a slight decrease in the pressure exponent from 0.84 to 0.75. However, we found that the burning rate of HMX/GAP propellant at 0.5 and 1 MPa did not depend on binder curing and particle size of fine HMX (less than 20 or 50 μm), and coincided with the data of Zenin [15] for cured propellant (fine fraction of HMX less than 50 μm). But the burning rates of the uncured propellants used in our study and in [3] are close to each other at 1 and 2 MPa but differ by a factor of 1.5 at a pressure of 0.5 MPa. The discrepancy in burning rate data of different authors can be attributed to a difference in the propellant compositions used. The burning rate depends on HMX particle size, on whether the propellant was cured, and on the elemental composition of the propellant. Data on the elemental composition of the propellant used in our study ($\text{C}_{17.1}\text{H}_{32.5}\text{N}_{27.2}\text{O}_{23.8}$) coincide with data of [4] ($\text{C}_{16.9}\text{H}_{31.7}\text{N}_{27.7}\text{O}_{23.7}$) and significantly differ in the hydrogen content from those presented in [3] ($\text{C}_{17.896}\text{H}_{21.811}\text{N}_{26.886}\text{O}_{24.156}$).

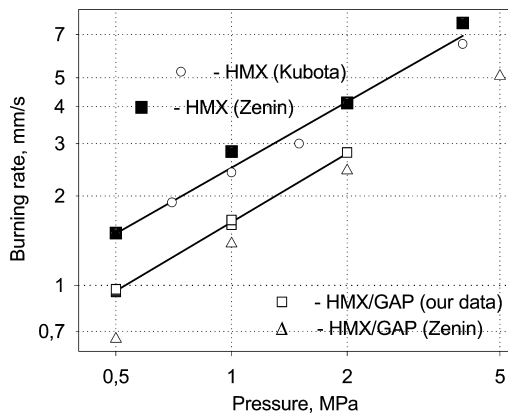


Fig. 1. Pressure versus burning rate for HMX/GAP propellant (uncured) and for pure HMX.

3.2. Temperature profile measurements

3.2.1. Effect of the particle size of the fine HMX fraction on the temperature profile of HMX/GAP flame at a pressure of 0.5 MPa

Temperature profiles (two profiles for each propellant) in HMX/GAP flame with different particle sizes of the fine fraction at 0.5 MPa are presented in Fig. 2. Replacement of HMX with particle sizes $\leq 20 \mu\text{m}$ (HMX₂₀/GAP propellant) by a fraction with particle sizes $\leq 50 \mu\text{m}$ (HMX₅₀/GAP propellant) did not change the temperature gradient near the burning surface up to a distance of 0.05 mm, but resulted in significant changes in the temperature profile at distances of $>0.05 \text{ mm}$.

3.2.2. Temperature profile in the HMX₂₀/GAP combustion wave at pressures of 0.5 and 1 MPa

Data on the thermal structure of HMX₂₀/GAP flame at a pressure of 1 MPa obtained in three experiments are presented in Fig. 3. The temperature profiles coincide with the data of [3] near the burning surface (up to 0.05 mm) and differ from them at larger distances. The maximum temperature $2600 \pm 100 \text{ K}$ in our experiment was attained at a distance of $\sim 0.7 \text{ mm}$. Thus, a 2-fold increase in the pressure (from 0.5 to 1 MPa) results in a decrease in the width of the HMX₂₀/GAP flame zone by a factor of ~ 1.6 .

Unlike in the experiments of [3], which showed the existence of an extensive plateau on the temperature profile of HMX/GAP flame at 0.5 and 1 MPa (at a temperature of $\sim 1300 \text{ K}$), no such plateau was found in our experiments (Figs. 2 and 3). But temperature profiles obtained at 0.5 MPa have a peculiarity at a distance from the burning surface from ~ 0.13 to 0.25 mm, which relates to a decrease in temperature gradient. With increase in pressure to 1 MPa, this peculiarity becomes less noticeable. In addition, the

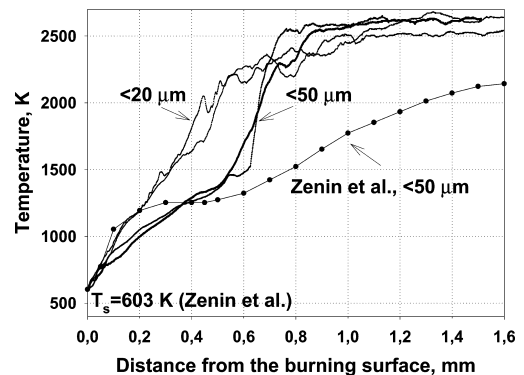


Fig. 2. Effect of the particle size of the fine HMX fraction on the temperature profile of HMX/GAP flame at a pressure of 0.5 MPa.

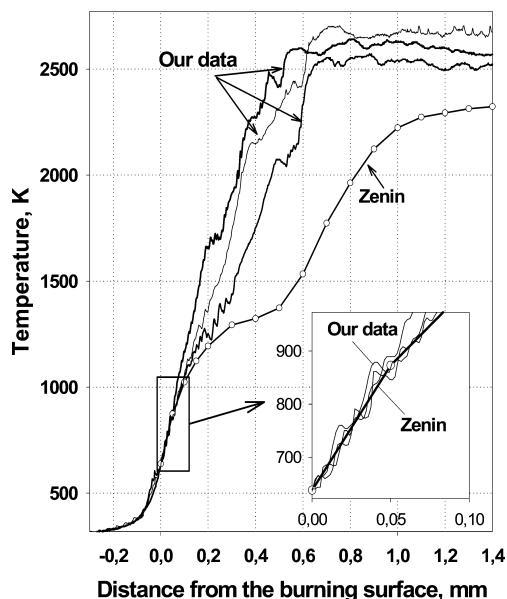


Fig. 3. Temperature profiles in an HMX₂₀/GAP combustion wave at a pressure of 1 MPa.

final temperature of combustion products was different: it was ~2600 K in our experiments at 0.5 and 1 MPa, 2170 K at 0.5 MPa, and 2320 K at 1 MPa in [3]. A possible reason for the difference between our data and the data of [3] is obviously connected with differences in GAP (elemental composition, enthalpy of formation) and propellant density. The density of the propellant used in [3] was 88% of the calculated maximum density versus ~98% in our case.

3.3. Chemical structure of HMX/GAP flame

Investigation of the chemical structure of un-cured composite HMX₂₀/GAP propellant was conducted in argon at pressures of 0.5 and 1 MPa using quartz Probes 1, 2, and 3. The composition of products near the burning surface at 0.5 and 1 MPa was measured using Probe 1 and Probe 2. The full flame structure was established at 0.5 MPa using Probe 3.

3.3.1. Composition of HMX/GAP combustion products at 0.5 and 1 MPa near and far from the burning surface

An analysis of samples taken from the flame identified the main species in the flame: H₂ (2), H₂O (18, 17), HCN (27, 26, 14), CO (28, 12), N₂ (28, 14), CH₂O (29, 30), NO (30, 14), CO₂ (44, 22), N₂O (44, 30, 28, 14), NO₂ (46, 30, 14), and HMX_v (75, 46, 42, 30, 29). The mass peaks used to identify species and determine their concentrations are shown in parentheses. Differentiation of species with the same mass-to-charge

ratio was performed using mass spectra of individual species obtained in calibrating experiments. The contributions of CO₂ and N₂O to mass peak 44 and the contributions of N₂ and CO to mass peak 28 were determined in the entire flame zone using mass peak 22 (CO₂⁺) and mass peak 14 (N⁺), respectively. The contributions of the remaining nitrogen species to mass peak 14 were subtracted from this peak before determination of N₂ concentration. The location of the burning surface was found from abrupt changes in most of the mass peak intensities at the moment of contact of the probe with liquid layer on the propellant surface. This was obviously related to density changes of the sampled products in a condensed to gas transition. In addition, the moment of contact of the probe with the burning surface was determined by video recording. Video recording was synchronized with mass spectrometric measurements in the same manner as in [7].

In addition, in a zone near the surface, mass peaks 39, 41, 42, and 43 were recorded. These peaks were not identified (except for part of mass peak 42, assigned to HMX vapor) but it was established that they decreased with increase in distance from the burning surface. We assume that the products of GAP combustion and/or thermal decomposition are responsible for these peaks. These peaks were not taken into consideration in the calculations of the combustion product composition. The compositions of HMX/GAP combustion products at pressures of 0.5 and 1 MPa at different distances from the burning surface are presented in Table 2. Averaged data on the concentration of products near the burning surface ($L = 0$ mm) obtained in two different experiments using Probe 2 are presented in Table 2. An increase in pressure from 0.5 to 1 MPa resulted in an increase in H₂ and CO concentrations near the burning surface and a decrease in NO and NO₂ concentrations. However, the HMX vapor concentration in products near the burning surface changed only slightly.

The composition of products near the burning surface of HMX/GAP propellant is not reproduced from experiment to experiment at a pressure of 0.5 MPa. The main difference observed is variation in the mole fraction of HMX_v from 0.1 to 0.27. Depending on the concentration variation of HMX vapor, the NO concentration varied from 0.24 to 0.10, the NO₂ concentration from 0.03 to 0.14, and the H₂O concentration from 0.20 to 0.06, respectively. The concentrations of the remaining products changed slightly. The main reason for this irreproducibility is probably the non-homogeneity of the burning surface, i.e., the presence of black particles on the burning surface revealed by video recording. These particles move slowly over

Table 2

Species concentration in flame of HMX/GAP propellant at 0.5 and 1 MPa at different distances from the burning surface (in mole fractions)

<i>L</i> (mm):	0	6	0	~1.2	Equil. ^a	0	~1.0	Equil. ^a
<i>P</i> (MPa):	0.1 ^b	0.1 ^b	0.5	0.5	0.5	1	1	1
<i>T</i> (K):	~700	—	603 ^c	2550 ^d	2594	638 ^c	2624 ^d	2608
H ₂	—	—	0.04	0.23	0.225	0.12	0.23	0.226
H ₂ O	0.10	0.10	0.14	0.12	0.115	0.16	0.12	0.116
HCN	0.26	0.04	0.13	0	<10 ⁻⁴	0.12	0	<10 ⁻⁴
N ₂	0.08	0.37	0.12	0.29	0.289	0.09	0.29	0.289
CO	0.07	0.35	0.02	0.34	0.335	0.12	0.34	0.336
NO	0.14	0	0.12	0	<10 ⁻⁴	0.08	0	<10 ⁻⁴
CH ₂ O	0.14	0.02	0.06	0	<10 ⁻⁴	0.04	0	<10 ⁻⁴
CO ₂	0.02	0.08	0.03	0.03	0.027	0.02	0.03	0.027
NO ₂	0.10	0	0.11	0	<10 ⁻⁴	0.05	0	<10 ⁻⁴
N ₂ O	0.07	0	0.04	0	<10 ⁻⁴	0.04	0	<10 ⁻⁴
HMX _v	—	—	0.18	0	0	0.17	0	<10 ⁻⁴

^a Equilibrium concentrations for H (0.007) and OH (7×10^{-4}) radicals are not presented in the table.

^b Data of laser-supported (100 W/cm²) combustion of propellant at 0.1 MPa from [4].

^c Surface temperature of propellant from [3].

^d Corrected for heat loss by radiation.

the burning surface and are probably partly decomposed GAP. Therefore, the observed irreproducibility of the composition of products near the burning surface is mainly due to the presence or absence of “GAP particle” on the burning surface near the tip of the probe. This implies that it is better to use averaged data on the composition of products near the burning surface for further application and validation of the HMX/GAP combustion model.

A comparison of our data on the HMX/GAP combustion product composition in self-sustained combustion at 0.5 and 1 MPa with the data of [4] on laser-supported combustion of HMX (75 μm)/GAP propellant in a laser heat flux of 100 W/cm² at 0.1 MPa shows that they are similar qualitatively but differ quantitatively. It is difficult to perform a reasonable quantitative comparison of the combustion product compositions near the burning surface obtained in our investigation and in [4] because of different experimental conditions. The main differences between our results and those in [4] are the absence of HMX vapor near the burning surface and the absence of H₂ in [4]. In [4], the measuring system did not allow detecting HMX vapor and hydrogen. The absence of HMX vapor in the data of [4] is probably due, on the one hand, to its decomposition or deposition on the inner wall of the microprobe. Another reason may be insufficient spatial resolution of sampling system used in [4], which did not allow correct measurements of products in a narrow zone 0.1 mm wide.

The composition of HMX/GAP combustion products at 0.5 and 1 MPa at a distance larger than 1.2 mm from the burning surface is very close to that at thermodynamic equilibrium (Table 2, equi).

3.3.2. Chemical structure of HMX₂₀/GAP flame at 0.5 MPa

An analysis of video records of the approach of the burning surface to Probe 3 at 0.5 MPa shows that a dark zone with an average width of 0.5 ± 0.1 mm exists near the burning surface of the propellant. The width of this zone was not constant during the propellant burning. On video records at 20-fold magnification, one can see the chaotic appearance of flame torches (3–5 torches simultaneously) with diameters of 0.5–1 mm on the burning surface. The lifetime of a single torch is less than 0.04 s. Black particles (slightly protruded over the burning surface) with sizes of 0.1–0.15 mm are also observed on the burning surface. These particles obviously are partly decomposed GAP. It is most likely that the formation of torches and temperature fluctuations are caused by the above-mentioned non-homogeneity of the burning surface. Therefore, the width of the dark zone obtained from temperature and concentration profiles in different experiments can differ within 0.4–0.6 mm.

The HMX₂₀/GAP flame structure at 0.5 MPa obtained using Probe 3 is presented in Fig. 4. The chemical and thermal structures shown in Fig. 4 were obtained in different experiments. The temperature profile in Fig. 4 is the result of averaging of the profiles presented in Fig. 2 and subsequent smoothing. The width of the zone of HCN and NO consumption obtained in mass spectrometric measurements coincides with the dark zone width measured using video recording. In the dark zone of width ~0.5 mm, two zones of chemical reactions were detected. In the first, narrow, zone 0.1 mm wide (adjacent to the burning surface), complete consumption of HMX_v and NO₂, and partial consumption of CH₂O with the

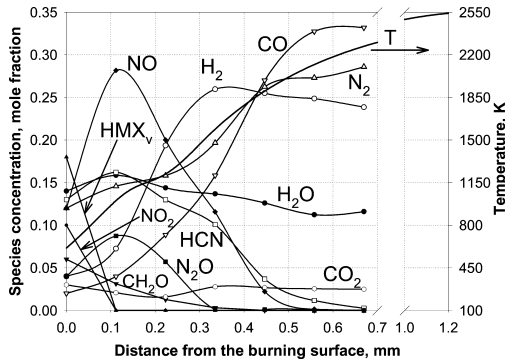


Fig. 4. Flame structure of HMX₂₀/GAP propellant at 0.5 MPa.

formation of NO, HCN, and N₂O occur. The concentrations of CO, N₂, and H₂ change only slightly. The temperature in this zone increases from 600 to ~970 K. Next, at a distance of 0.1–0.5 mm, consumption of N₂O, CH₂O, HCN, and NO with the formation of H₂, CO, and N₂ takes place. The temperature increases from 970 to 2000 K. Thus, the NO, HCN, and N₂O concentration profiles reach a maximum at $L \sim 0.12$ mm. At distances larger than 0.5 mm, a luminous zone begins, in which there is further consumption of HCN. In the experiment whose results are presented in Fig. 4, concentration profiles were measured only to ~0.7 mm. At this distance, HCN is not completely consumed, and the temperature reaches ~2300 K. In the experiments in which flame structure was investigated at large distances from the burning surface, the width of the HCN consumption zone was significantly greater than those of the remaining products and was equal to ~1.0 mm. The H₂O and CO₂ concentrations changed slightly in the whole flame zone. The H₂ concentration reaches a maximum at $L = 0.35$ mm, whereas CO and N₂ concentrations are maximized at $L = 0.55$ mm. A possible reason for this is that the diffusion coefficient of H₂ is higher than those of remaining combustion products. Element content profiles in HMX/GAP propellant flame at 0.5 MPa calculated without accounting for diffusion fluxes of species are presented in Fig. 5. The maximum deviations of N and H contents are ~25–30%. The oxygen content coincides with the initial amount over the entire flame zone. The largest deviation (~40%) from the initial element content is observed for carbon. In a zone ~0.1 mm wide adjacent to the burning surface, there is a steep gradient of species concentrations; therefore, the element content in this zone can differ from the initial one. However, the concentration gradient decreases at distances larger than 0.1 mm but the amounts of C, H, and N still differ from the initial ones. It can be assumed that a decrease in the amounts of C and H

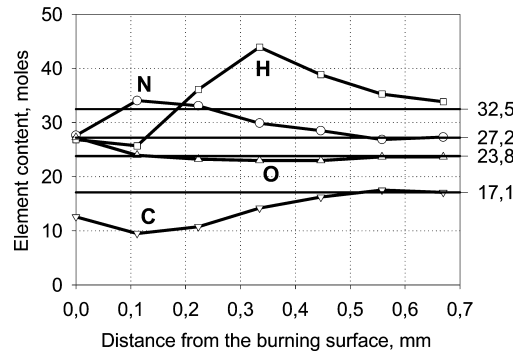


Fig. 5. Element content profiles in HMX/GAP propellant flame at 0.5 MPa (without accounting for diffusion fluxes of species).

near the burning surface is due to the presence of unidentified gaseous products of GAP gasification. This assumption explains the nature of the dependence of C and H content on the distance from the burning surface.

In spite of different experimental conditions used in our investigation of self-sustained HMX/GAP combustion at 0.5 MPa and in laser-assisted combustion (100 W/cm²) at 0.1 MPa in [4], the behavior of species concentration profiles is similar. The width of the dark zone in self-sustained combustion is about an order of magnitude smaller than that in laser-assisted combustion. In addition, in the case of self-sustained combustion, a plateau is absent on species concentration profiles.

4. Conclusions

1. Eleven species H₂, H₂O, HCN, N₂, CO, NO, CH₂O, N₂O, NO₂, CO₂, and HMX vapor were identified, and their concentrations were measured in a zone adjacent to the burning surface at pressures of 0.5 and 1 MPa. At a pressure of 0.5 MPa, the composition of products near the burning surface of HMX/GAP propellant is not reproduced from experiment to experiment. However, for averaged data on species concentrations near the burning surface the following trend was observed: an increase in the pressure from 0.5 to 1 MPa resulted in an increase in H₂ and CO concentrations, and a decrease in NO and NO₂ concentrations.
2. Species concentration profiles in the flame of self-sustained HMX/GAP combustion at 0.5 MPa were measured. In the first narrow zone 0.1 mm wide, complete consumption of HMX vapor and NO₂, and partial consumption of CH₂O with the formation of NO, HCN, and N₂O occur. In the second zone

- 0.4 mm wide, the consumption of NO, HCN, N₂O, and CH₂O with the formation of the final products (H₂, CO, N₂, and CO₂) takes place.
- Temperature profiles in the combustion wave of HMX/GAP propellant at 0.5 and 1 MPa were measured. An extensive plateau on the temperature profiles was not observed. The data obtained differ from available literature data, probably because of a difference in the properties of GAP used in the propellant.
 - A comparison of flame structure in self-sustained HMX/GAP combustion at 0.5 MPa with similar data for laser-supported combustion of the same propellant at 0.1 MPa shows that they are similar qualitatively but differ quantitatively.
 - The data obtained can be used to develop and validate a self-sustained combustion model for propellants based on HMX and GAP.

Acknowledgment

This research is supported by US Army Research Office under Grant DAAD19-02-1-0373.

References

- [1] N. Kubota, T. Sonobe, *Proc. Combust. Inst.* 23 (1990) 1331–1337.
- [2] E.S. Kim, V. Yang, Y.-C. Liao, *Combust. Flame* 131 (3) (2002) 227–245.
- [3] A.A. Zenin, S.V. Finjakov, *Synthesis, Production and Application*, Fraunhofer Institut Chemische Technologie, DWS Werbeagentur und Verlag GmbH, Karlsruhe, Germany, 2002, p. 6-1.
- [4] T.A. Litzinger, Y. Lee, C.-J. Tang, in: V. Yang, T.B. Brill, W.-Z. Ren (Eds.), *Solid Propellant Chemistry, Combustion, and Motor Interior Ballistics*. American Institute of Astronautics and Aeronautics, Reston, 2000, p. 335.
- [5] T.A. Litzinger, B.L. Fetherolf, Y.-J. Lee, C.-J. Tang, *J. Propul. Power* 1 (4) (1995) 698–703.
- [6] C.-J. Tang, Y.-J. Lee, G. Kudva, T.A. Litzinger, *Combust. Flame* 117 (1–2) (1999) 170–188.
- [7] O.P. Korobeinichev, in: V. Yang, T.B. Brill, W.-Z. Ren (Eds.), *Solid Propellant Chemistry, Combustion, and Motor Interior Ballistics*. American Institute of Astronautics and Aeronautics, Reston, 2000, p. 335.
- [8] G. Krien, H.H. Licht, J. Zierath, *Thermochim. Acta* 6 (5) (1973) 465–472.
- [9] R.M. Fristrom, *Flame Structure and Processes*. Oxford University Press, New York, USA, 1995.
- [10] A.A. Zenin, *Experimental Investigation of the Burning Mechanism of Solid Propellants and Movement of Burning Products*, Ph.D. dissertation, Institute of Chemical Physics, USSR Academy of Sciences, Moscow, USSR, 1976.
- [11] A.G. Tereshenko, O.P. Korobeinichev, A.A. Paletsky, L.T. DeLuca, *Rocket Propulsion: Present and Future*, Politecnico di Milano, grafiche g.s.s., 2003, Pozzuoli, Naples, Italy, 2002, pp. 24–31.
- [12] O.P. Korobeinichev, L.V. Kuibida, A.A. Paletsky, A.G. Shmakov, *J. Propul. Power* 14 (6) (1998) 991–1000.
- [13] G.B. Belov, *Propell. Explos. Pyrot.* 23 (1998) 86–89.
- [14] R. Behrens Jr., *Int. J. Chem. Kinet.* 22 (1990) 135–157.
- [15] A.A. Zenin, *Study of Combustion Mechanism of Nitramine–Polymer Mixture*, Report No. R&D 8724-AN-01, European Research Office of the US Army, 2000.

Comment

Kenneth Kuo, Penn State University, USA. Would you please indicate the type of material used in your probe tip? Could the probe material introduce some catalytic effects?

Reply. “Sonic” probes made of quartz were used for sampling. It is possible that the material of probe render

some catalytic effects. However, the skimmer, located behind the probe, collects only the central portion of the supersonic jet, which is free of heterogeneous reactions on the inner walls of the probe.